Fisheries Research 168 (2015) 72–84

Contents lists available at ScienceDirect

Fisheries Research

journal homepage: www.elsevier.com/locate/fishres

Selectivity and two biomass measures in an age-based assessment of Antarctic krill (*Euphausia superba*)

Douglas Kinzey*, George M. Watters, Christian S. Reiss

Antarctic Ecosystem Research Division, Southwest Fisheries Science Center, NOAA National Marine Fisheries Service, 8901 La Jolla Shores Drive, La Jolla, CA 92037, USA

ARTICLE INFO

Article history:
Received 28 January 2015
Received in revised form 27 March 2015
Accepted 28 March 2015
Handling Editor A.E. Punt
Available online 22 April 2015

Keywords:
Survey selectivity
Integrated modeling
Simulation testing
Acoustic biomass
Net biomass

ABSTRACT

An integrated, age-structured model was fitted to different combinations of survey data using two forms of selectivity (logistic or double-logistic) with time-constant or annually varying selectivity to investigate the population dynamics of Antarctic krill (*Euphausia superba*) near the Antarctic Peninsula. The data were from surveys conducted by the U.S. Antarctic Marine Living Resources Program around the South Shetland Islands from 1992 to 2011. Two indices of krill biomass based on (1) trawl-net samples and (2) hydroacoustic sampling were combined with length-compositions from the nets. Sixteen model configurations using different combinations of the two biomass surveys with the various options for modeling selectivities were examined. Parameters were estimated in phases with the sequential order of the phases randomized until an invertible Hessian matrix was obtained. Model consistency for the estimates of derived quantities was tested using simulated data. Annual trends in the estimates of total biomass, spawning biomass, and recruitment were similar among different configurations assuming time-constant selectivity, but the absolute scaling ranged widely depending on which biomass indices were used. All configurations with time-constant selectivities were able to reproduce the derived quantities of the operating model when fitted to simulated data. Annually varying selectivities produced more variable estimates of the trends in population biomass, but less variable estimates of scale, compared to time-constant configurations fitted to the same data. The models with annually varying selectivities did not produce invertible Hessian matrices, and four of these configurations could not reproduce the derived parameters of their operating model when fitted to simulated data. Using AIC, the model with logistic, time-constant selectivities was selected as the best configuration to fit both sources of biomass data. The two-stage approach of first randomizing the phase order until an invertible Hessian matrix is achieved and then verifying the reproducibility of the estimates of derived quantities using simulated data could be employed in any integrated stock assessment with parameters estimated in phases.

1. Introduction

Antarctic krill (*Euphausia superba*, hereafter krill) have a circumpolar distribution (Siegel, 2005; Hofmann and Hüsrevoğlu, 2003; Atkinson et al., 2009). The multinational fishery for krill is regulated by the Commission for the Conservation of Antarctic Marine Living Resources (CCAMLR). At present, krill catches are about 200,000 tons yr^{-1}, and there is interest in increasing this catch (Nicol et al., 2012). In recent decades, the catches have been from the Scotia Sea (Fig. 1), and annual removals are believed to be less than 1% of the 60.3 million tons (mt) standing stock estimated from a multinational acoustic survey conducted by Members of CCAMLR in 2000, referred to as the "CCAMLR 2000 Survey" (Hewitt et al., 2004; CCAMLR, 2010).

The total catch limit of krill from the Scotia Sea (5.61 mt) was established using the "generalized yield model", an age-structured simulation model (Constable and de la Mare, 1996; Constable et al., 2003; CCAMLR, 2010). This model does not statistically connect a model to data using a likelihood function, but instead treats all inputs for a single simulation as known (Kinzey et al., 2013). Variability among simulations is represented as process error, with recruitments for each simulation randomly selected from a pre-defined probability distribution. Each single simulation is deterministic. Quantities of interest (e.g., spawning biomass) are calculated from many thousands (typically 10,000) randomized

* Corresponding author. Tel.: +1 858 546 5601.
E-mail addresses: Doug.Kinzey@noaa.gov (D. Kinzey), George.Watters@noaa.gov (G.M. Watters), Christian.Reiss@noaa.gov (C.S. Reiss).

http://dx.doi.org/10.1016/j.fishres.2015.03.023

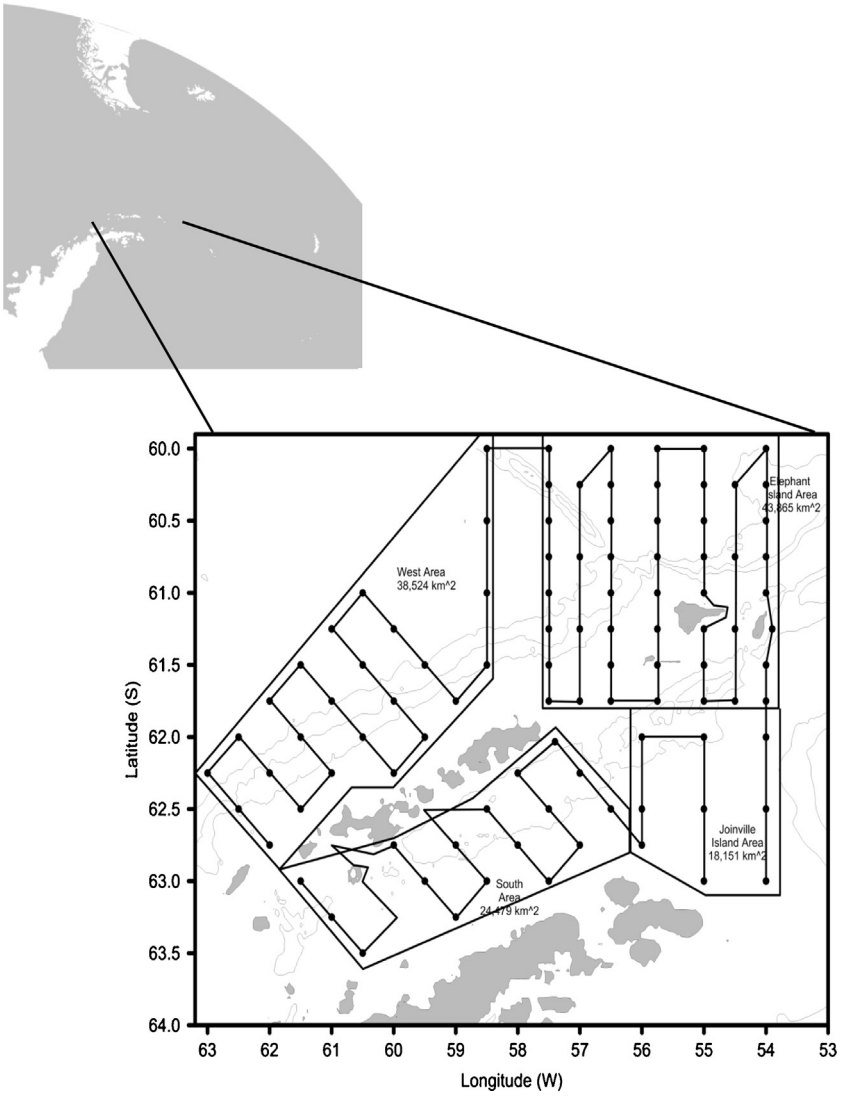

Fig. 1. The U.S. AMLR study area in the Scotia Sea between South America and the Antarctic Peninsula. Survey strata are defined by polygons enclosing several acoustic transects and net-tow stations.

replicates, and statistics of these quantities (e.g., the median spawning biomass) are compared to decision criteria that are considered to be precautionary. Precautionary catch limits are those that meet the decision criteria based on the simulation results.

The objectives of this paper are threefold. First, we aim to develop a statistical modeling framework to assess the status and productivity of Antarctic krill in the Scotia Sea. Second, we conduct a general examination of the effects of different structural assumptions about the forms of selectivity for different data sources. Our third objective is to develop procedures that improve the ability to achieve convergence in integrated stock assessments employing complex, nonlinear likelihood models with mixed data sources. We evaluate the effects of combining or ignoring separate biomass indices (from net trawls and hydroacoustics), allowing selectivity to either vary annually or be time-constant. We use 20 years of survey data on Antarctic krill from around the Shetland Islands in the Antarctic Peninsula.

The models described here do not include fishery-dependent data. To date, catches taken by the krill fishery are believed to be a small fraction of the total krill population in the Scotia Sea and are thus expected to have minimal effect at the population level. Fishery catches and size-composition data will be incorporated into future models to compare projected outcomes from increasing catches to the CCAMLR decision rules. At this stage of development, however, our aims are to evaluate the internal consistency of the model estimates when fitting to different sources of survey data using different assumptions about selectivity, and increase the prospects of achieving model convergence through the use of randomized phase sequences.

2. Materials and methods

The biomass density of Antarctic krill ($g\,m^{-2}$, or equivalently, tons km^{-2}) in the Scotia Sea has been measured using samples from zooplankton nets and acoustic backscatter methods. While there is overlap in the resulting biomass values produced using the two methods, nets often produce biomass densities at the lower end of those produced using acoustics. Previous studies comparing estimates of the biomass density of krill from zooplankton nets and acoustic methods have noted several issues (Everson, 1982; Hewitt and Demer, 1996; Wiebe et al., 2004, 2011; Hewitt et al., 2003; Fielding et al., 2004, 2012; Reiss et al., 2008; Atkinson et al., 2009). Krill of different sizes may differ in net-avoidance capabilities. Krill size, density within aggregations, and swimming orientation affects their acoustic target strength. Diurnal migrations can move krill above the range susceptible to acoustic observation so that

Table 1
Availability of net and acoustic biomass indices from the U.S. AMLR surveys by year, stratum, and leg. "J" indicates January, and "F" indicates February sampling legs. Legs without asterisks have only net tows; legs with asterisks have both net tow and acoustic biomass indices. See Fig. 1 for a map of the survey strata.

	Elephant Island	Joinville	Southern	Western
1992	J,F			
1993	J		J	J
1994	J,F		J,F	J,F
1995	J,F		J,F	J,F
1996	J*,F*		J,F	J,F
1997	J*	J	J*	J
1998	J*,F*		J*,F*	J*,F*
1999	J*,F*		J*,F*	J*,F*
2000	F*	F	F*	F*
2001	J*,F*		J*,F*	J*,F*
2002	J*,F*	J*,F*	J*,F*	J*,F*
2003	J*,F*	J,F	J*,F*	J*,F*
2004	J*,F*	J*,F*	J*,F*	J*,F*
2005	J*,F*	J*,F*	J*,F*	J*,F*
2006	J*	J	J*	J
2007	J*	J	J*	J
2008	J*,F*	J*	J*,F*	J
2009	J*	J*	J*	J
2010	J*	F*	J,F*	J,F*
2011	J*,F*	J*,F*	J*,F*	J*

Table 2
Annual sampling effort for nets (number of tows, volume of water sampled integrated over depth) and acoustics (number of transects, nautical miles).

Year	Net sampling		Acoustic sampling	
	N tows	Volume/depth (m^2)	N transects	Nautical miles
1992	113	2826.5		
1993	79	1945		
1994	123	2725.3		
1995	148	3825.6		
1996	167	4157.8	18	1347
1997	95	1959.4	16	972
1998	187	4731.9	48	2347
1999	86	1986.7	33	1750
2000	75	1864.2	18	956
2001	167	3959.5	40	2457
2002	125	2747.3	41	2159
2003	165	3830.9	39	1890
2004	150	3455.3	43	2390
2005	160	3309.2	44	2156
2006	84	1781.2	21	1002
2007	91	2023.5	21	1238
2008	135	3426	35	2062
2009	86	2583.6	23	1375
2010	61	1266.7	17	757
2011	116	3029.7	30	1439

daytime and nighttime biomass indices in the same area can differ substantially. Krill acoustic target-identification windows are difficult to verify and can vary seasonally and annually.

In this study, disparities in the time series of biomass indices from nets and hydroacoustics will be modeled as differences in age-based selectivity. The estimation of selectivity in integrated fisheries models is an effort to reconcile the observed size- or age-structure in a time series of sample data with the cohort structure required to maintain a self-consistent model of population dynamics. Differences in the probabilities of being sampled at different ages or life stages can bias the results from population models if such differences are not modeled explicitly.

2.1. Field survey design

Annual surveys to sample krill in the South Shetland Islands during the austral summer were conducted by the U.S. Antarctic Living Marine Resources (AMLR) Program of the National Marine Fisheries Service, Southwest Fisheries Science Center, over the 20-year period between 1992 and 2011 (Reiss et al., 2008; Table 1, Fig. 1). Sampling effort varied from 61 to 187 net tows and from 16 to 44 acoustic transects per year (Table 2). Estimates of krill biomass based on these survey data provide two series of annual biomass indices, one from acoustics and one from nets. Annual length-compositions of krill (proportions-at-length in 1 mm bins) were sampled from the nets during all years.

The U.S. AMLR surveys sampled acoustic backscatter at frequencies of 38, 120, and 200 kHz, and the annual size distributions and densities of krill vulnerable to the nets. Acoustic backscatter was integrated over depths from 10 to 250 m, while the net data sampled the densities of identified krill in 1 mm size bins over depths from the surface to 170 m.

The total area covered by the U.S. AMLR survey grid is ~125,000 km^2, about 6% of the area covered by the CCAMLR 2000 Survey. Initially, the U.S. AMLR surveys focused on a central region surrounding the Elephant Island and collected data using one or two frequency hydroacoustics and net trawls. Sampling coverage in 1992 occurred only in the Elephant Island portion of the grid during two legs. The spatial extent of the sampling was expanded after 1992 to include three additional strata, labeled "West" (western side of South Shetland Islands), "South" (Bransfield Strait) and "Joinville" (waters between Elephant Island and Joinville Island at the northern tip of the peninsula). From 1993 to 2011, at least three of the four strata were sampled every year for one or two legs. Sampling was conducted in two legs most years after 1992, a January leg and a February leg, although not every station or stratum was sampled during all years. After 1995, the surveys incorporated simultaneous 3-frequency acoustic sampling of krill along transects between net stations. Acoustic samples at less than 3-frequencies are not used here, so that from 1992 to 1995 only data from net tows are fitted by the models. After 1996, biomass indices from both 3-frequency acoustics and nets were available for every year (Table 1).

2.2. Model framework

The length-composition data (from nets) and the two biomass indices (from acoustics and nets) were fitted using an age-based, integrated assessment model developed in AD Model Builder (Fournier et al., 2012). Model equations are provided in Appendix. Cohort abundance-at-age is determined by initial recruitment with subsequent, annual decreases due to total mortality (App. Eq. (A.1)). At present, total mortality includes some fishing mortality but this will be separated from natural mortality once fisheries data are incorporated into the model. The model operates on an annual time step but can represent survey results at smaller time scales such as by month or season using fractions of the year. The model can also represent spatially disaggregated survey data. Here we combined the annual data from all survey months and strata, but the results were qualitatively similar when estimates were disaggregated by month and stratum.

Antarctic krill are spawned from January to March and spend their first year as larvae, developing to juveniles that are about 18 mm in length by the end of the year (Siegel and Loeb, 1995). The larval stage was not included in the model. Recruitment in the model begins at age 1, with juvenile krill.

Laboratory studies have demonstrated that krill can live more than 9 years (Ikeda and Dixon, 1987 cited in Nicol, 2006). The model has 10 ages, with age 10 being a plus group. The model estimates spawning biomass starting in 1982, 10 years before the first length-composition data used here were observed. This allows the estimated length frequencies for all 10 cohorts to fit the first year of observed length-compositions in 1992. The estimates for these "pre-data" years are less reliable than for the more recent years with

both length-compositions and biomass indices (starting in 1992 for nets and 1996 for acoustics). Parameter estimates from the pre-data years will typically have wider uncertainty bounds than from more recent years.

The slope and position parameters for selectivities, for both logistic selectivity (β and α in Eq. (A.2)), and double-logistic selectivity (Λ, ϖ, Ψ, τ in Eq. (A.3)) were unconstrained. Data were weighted in the likelihood (Eq. (A.4)) by standard errors of the log-normally distributed biomass indices and by effective sample sizes for the multinomially distributed length frequencies (Eq. (A.5)). Standard errors for the net-based biomass indices were calculated using individual hauls in a year as replicates, and, for the acoustic indices, methods described by Jolly and Hampton (1990). Effective sample sizes for the length-compositions were the numbers of net samples taken each year (Table 2). Survey catchabilities were bounded as a logistic function between 0 and 1.

Numbers-at-age in the model were converted to numbers-at-length (mm) using a von Bertalanffy growth relationship with estimated parameters L_∞, k, and σ_v (Eq. (A.6)). This length-at-age relationship, mediated by survey catchability and selectivity (Eqs. (A.2) and (A.3)), was used to compare survey biomasses with model estimates of vulnerable biomass (Eq. (A.4)). Weight-at-length was assumed known and calculated using Eq. 3 from Hewitt et al. (2004) ($W(L) = 2.236 \times 10^{-6} L^{3.314}$).

Recruitment was estimated as normally distributed, annual deviations from a mean value (Eq. (A.1)). This produced a parameter estimate for each year with observed data, as well as an additional parameter for the mean recruitment. Deviations from Beverton–Holt spawner–recruit predictions in the estimated recruitment deviations were penalized (Eq. (A.7)), as was the total variation among recruitment deviations (Eq. (A.8)). This method of penalizing departures from a parametric Beverton–Holt relationship centers the estimated recruit abundances around the expectations of the Beverton–Holt while allowing for recruitment variability even at high values of spawning biomass relative to unfished spawning biomass (B_0) and steepness (h). Steepness, the proportion of unfished recruitment that would be achieved at 20% of unfished spawning biomass, was bounded between 0.21 and 1. The penalty on annual departures from Beverton–Holt recruitment trends effectively decreased as the estimates for steepness increased, although the mean recruitment was maintained near that expected by the mean Beverton–Holt prediction (Eq. (A.7)).

Early model runs indicated the recruitment deviation σ^R was not estimable, thus it was pre-specified to be 0.9 based on fits to the data (most configurations had lower objective values with an assigned σ^R of 0.9 than with assigned values between 0.6 to 0.8 or than with values of 1.0 or greater).

The parameter for mortality (M) combines the net effects of total mortality with immigration and emigration. Parameter estimates for mortality can be either unconstrained or penalized for departures from a pre-specified value (Eq. (A.9)). In this study, the logarithm of M was initially estimated and then exponentiated before use. Departures of the estimate of M from 1.0 (e^0) were penalized with a standard error of 2.7 (e^1) (App. Table A.1).

2.3. Model configurations

The effects of fitting to different biomass indices were investigated by using either net-based or acoustic-based indices in separate models, or with both types in a single model. The model framework allows the parameters for age-based selectivity to be estimated separately for each survey. In this framework, a survey is defined as a spatial or temporal grouping of samples assumed to have the same selectivity. Example groupings could be net tows by year, month, or survey stratum. Acoustic surveys may be similarly aggregated at various temporal or spatial scales. For this study, the net and acoustic data were grouped temporally into annual samples and spatially as a single area to produce two annual surveys, "nets" and "acoustics". All model configurations used the same annual length-composition data from the nets.

Table 3
Eight model configurations using different biomass indices and form(s) of selectivity. These eight configurations were fitted assuming both time-constant and annually varying selectivities (for a total of 16 configurations).

Configuration[a]	Description
a-l	Acoustic-only biomass, logistic selectivity
a-d	Acoustic-only biomass, double-logistic selectivity
n-l	Net-only biomass, logistic selectivity
n-d	Net-only biomass, double-logistic selectivity
b-ll	Both biomasses, both logistic selectivity
b-ld	Both biomasses, acoustics logistic, nets double-logistic
b-dl	Both biomasses, acoustics double-logistic, nets logistic
b-dd	Both biomasses, both double-logistic selectivities

[a] Type(s) of biomass data indicated as "a-", "n-", and "b-" representing whether biomass was indexed using acoustic data only, nets only, or both sources combined in the same model, with logistic or double-logistic selectivities as indicated by "l" or "d", respectively.

Configurations differed by the type(s) of biomass index used (nets only, acoustics only, both types), whether selectivity was modeled as logistic or double-logistic, and whether selectivity was constant over time or varied by year (Table 3). Configurations using different types of data are not statistically comparable. Configurations based on the same data but with different forms of selectivity are comparable. Models using the same data were ranked using the Akaike Information Criterion (AIC; Burnham and Andersen, 1998).

When nets and acoustics were combined in a configuration they were treated as two surveys with separate selectivity parameters. Surveys were either assigned the same form of selectivity, or different forms. The numbers of parameters estimated by the different configurations with time-constant selectivity ranged from 41 to 46. The numbers of parameters estimated by configurations with annually varying selectivity ranged from 79 to 200.

Different forms of selectivity have different implications for the underlying population processes being modeled. Double-logistic selectivity allows for decreased vulnerability of older age classes, which could be the case if older animals are located inside the area sampled but are less available to the sampling gear due to behavioral or other causes, or are located outside of the areas sampled due to factors such as depth or movement with age. Some studies have suggested that from 2 to 20% of Antarctic krill, including gravid females, may be located at depths from 200 to 3500 m, feeding on the seabed as well as in the water column (Clarke and Tyler, 2008; Brierley, 2008; Schmidt et al., 2011) although other studies suggest the proportions of krill at depths below 200 m are only a couple of percent (Atkinson et al., 2009; Siegel et al., 2013). The logistic assumption, in which selectivity increases monotonically with age, does not allow for such "cryptic biomass" of older individuals. This might be the case if the spawning biomass responsible for the recruitment was entirely inside the area sampled. With the appropriate parameter values, the double-logistic form of selectivity can reproduce the logistic form so, in theory, if the logistic shape best fits the data a double-logistic model should produce a logistic relationship.

The expectation for configurations with annually varying selectivities, following Lee et al. (2014) and Francis (2011), is that the influence of the length-composition data on the model estimates of scaling parameters such as unfished recruitment or spawning biomass will be reduced relative to the models with time-constant selectivity. Providing more selectivity parameters allows the length-compositions to be fitted more easily and so reduces their influence on the model estimates.

Table 4
Potentially estimated parameters and their phases. The number of parameters estimated is one per survey for parameters subscripted with an *s* and one per year for parameters subscripted with a *y*.

Description	Phase	Parameter
Natural mortality	phase_M	M
von Bertalanffy maximum expected length	phase_al	L_∞
von Bertalanffy slope	phase_al	k
von Bertalanffy standard error	phase_al	σ^v
Unfished mean recruitment	phase_Rzero	R_0
Mean recruitment	phase_meanRec	$\ln(\bar{R})$
Beverton–Holt recruitment	phase_srec	$\hat{R}_y$
Annual deviations around mean recruitment	phase_srec	$\ln(\varepsilon_y^R)$
Steepness	phase_srec	h
Survey catchability	phase_q_srv	q_s
Ascending slope of logistic or double-logistic selectivity	phase_sel_srv	β_s or Λ_s
Descending slope of double-logistic selectivity	phase_sel_srv	ϖ_s
Age at midpoint of logistic or increasing slope of double-logistic selectivity	phase_sel_srv	α_s or Ψ_s
Factor added to Ψ_s for age at midpoint of decreasing double-logistic selectivity	phase_sel_srv	τ_s

2.4. Randomized phases

Subsets of the parameters were estimated in phases during optimization, holding some parameters at initialized values while others were estimated in an early phase, then estimating those initially held constant in subsequent phases. All previously estimated ("active") parameters continued to be re-estimated in subsequent phases once they were activated. This process can allow complex nonlinear models to be optimized when not all parameters can initially be estimated at the same time (Fournier et al., 2012). Parameters were grouped into seven subsets of phases for optimization (Table 4). Survey q and selectivity were estimated with separate phases for each biomass index (e.g., when two biomass indices were included, there were two phases for q and two phases for selectivities), for a total of nine possible sets of phase order (over 360 thousand unique arrangements) for some configurations. The order in which each subset of parameters was estimated was assigned randomly until the optimization procedure produced a positive-definite Hessian matrix. The inverse of the Hessian matrix approximates the variance–covariance matrix for the parameters, thus allowing asymptotic variance estimates and Markov chain Monte Carlo (MCMC) sampling.

2.5. MCMC sampling and simulated data

Markov chain Monte Carlo sampling of spawning biomass, recruit abundance, and "mortality" was conducted for each model configuration to illustrate the effects of the assumptions represented by different model configurations. Models were run for 5,000,000 MCMC iterations, sampling every 1000th value. These chains provided a way to compare the absolute scaling and time series patterns in the estimates from different configurations. The purposes of conducting these MCMC samples were to confirm that an invertible Hessian had been obtained (some configurations that produced asymptotic variance estimates were unable to be sampled using MCMC) and to give an indication of the central tendency of the estimates rather than to fully characterize uncertainties.

An additional evaluation of model convergence is to assemble a simulated data set from a generating model with a positive definite Hessian matrix (the "operating model") and then ensure that a new model (the "estimating model") using this simulated data fits the simulated data and reproduces the derived quantities of the operating model. This procedure has been termed a "self-test" (Deroba et al., 2015). Simulated data were calculated for each model configuration. The generating model configuration was then refitted to the simulated data to evaluate estimates of spawning biomass, recruitment, natural mortality, and steepness against mathematically consistent "truths" that were known.

Using the same model to generate its own data eliminates the issue of model-misspecification when evaluating the results (Lee et al., 2011). The simulated data are consistent with the likelihood instead of being produced by natural processes for which appropriate likelihoods are incompletely known or by another model with a different likelihood structure. Using the same model to estimate derived quantities from data that it generated can indicate a lack of convergence or other issues if the estimates using simulated data do not match those of the original generating model.

Simulated data were provided for every year of the time series represented by each model. Similarly to the development of the models based on the field data that generated the simulated data, the estimating models using simulated data also used randomized phase sequences to find the best fits. All parameters estimated in the original generating models (Table 4) were re-estimated by models using the simulated data.

2.6. Density ranges for the Scotia Sea and in the U.S. AMLR survey area during the CCAMLR 2000 Survey

Reported densities of krill throughout the Scotia Sea during the CCAMLR 2000 Survey ranged from 0.05 to 757.7 g m^{-2} (for individual acoustic transects), or from 1.82 to 319.42 g m^{-2} (when transects were averaged by survey strata). The mean density among CCAMLR 2000 transects around the Antarctic Peninsula (including transects outside the U.S. AMLR survey area) was 19.6 g m^{-2}, and the mean density for the entire Scotia Sea was 29.2 g m^{-2} (Tables 3 and 4 in Fielding et al., 2011).

For comparison with U.S. AMLR biomass indices (App. Table A.2), a mean biomass was calculated from the CCAMLR 2000 transects that were located inside the U.S. AMLR survey area. There were 11 such transects, labeled AP11 to AP19 and SSI01 to SSI07 (Trathan et al., 2001; Fielding et al., 2011). Transect-specific estimates of krill density were weighted by transect length from Table 2 in Fielding et al. (2011) to calculate estimates of density (71.7 g m^{-2}) and biomass (8.96 mt) from the CCAMLR 2000 Survey inside the U.S. AMLR study area.

Total biomass estimates from the model configurations fitted here to the U.S. AMLR data from 1992 to 2011 were converted to densities and compared to the range of densities for individual transects throughout the Scotia Sea during CCAMLR 2000 Survey. The model estimates of biomass were converted to densities in two ways, based on different assumptions about the area in which the total population being modeled resides. In the first calculation, the population biomasses from the models were assumed to exist entirely inside the U.S. AMLR survey area (125,019 km^2). In the second calculation, densities were calculated assuming the population biomass represented by the models was located throughout the

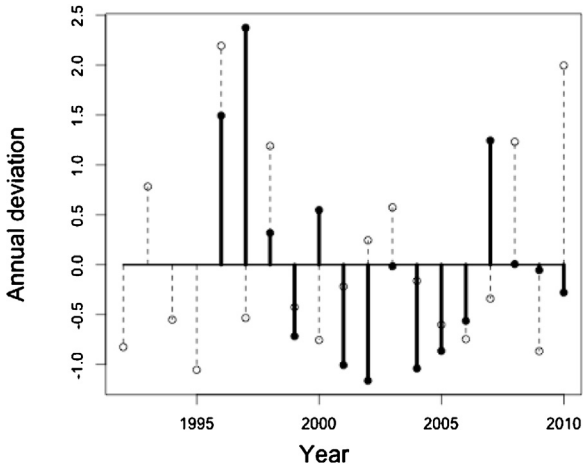

Fig. 2. Annual, normalized standard deviations from mean values for net (dashed lines) and acoustic (solid) biomass indices.

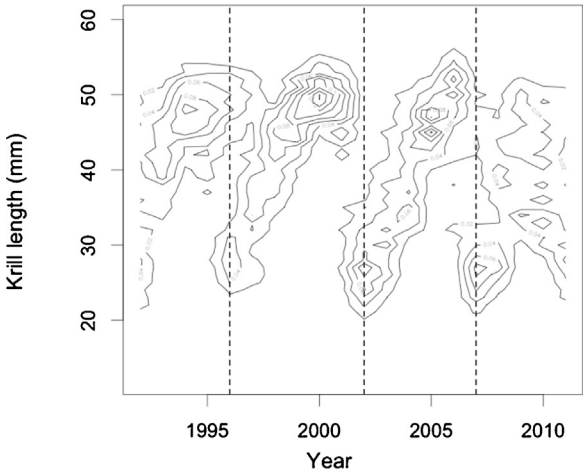

Fig. 3. Annual length compositions of krill surveyed by the U.S. AMLR Program from 1992 to 2011. Isopleth lines indicate values from 0.02 to 0.08. Dashed vertical lines were drawn by eye to indicate years with high proportions of small krill.

Scotia Sea (2,065,244 km^2). The actual population supplying the area sampled in the U.S. AMLR surveys is probably distributed over an area somewhere between these two extremes, but this approach might bracket plausible spatial boundaries for the total population of krill that is surveyed by the U.S. AMLR Program.

3. Results

3.1. Biomass indices and length-frequencies

Annual biomass densities of krill measured acoustically were usually greater than biomass densities measured with nets for the same years (Table A.2). The annual biomass densities derived from U.S. AMLR net tows during 1992 to 2011 ranged between 1.8 and 10.3 g m^{-2} and from acoustics during 1996 to 2011 between 2.2 and 46.5 g m^{-2} (Table A.2). Mean annual densities were 4.6 g m^{-2} (SD 2.6) from nets and 16.8 g m^{-2} (SD 12.5) from acoustics. These values were less than the 71.7 g m^{-2} calculated using CCAMLR 2000 acoustic transects inside the U.S. AMLR survey area and for most years were less than the 29.2 g m^{-2} calculated during CCAMLR 2000 for the entire Scotia Sea survey (Fielding et al., 2011). These are direct extrapolations from the observed data without accounting for potential selectivity.

In addition to differences in overall scaling, the biomass indices from nets and acoustics presented different annual dynamics (Fig. 2). These two methods of measuring krill biomass were not correlated (Pearson's $r = 0.17$). To check whether the two biomass indices tracked different ages (sizes) of krill, correlations between them were examined at lags of up to 3 years. Correlations between the two indices remained low for the lagged data. The highest correlation, 0.35, was achieved when the net biomass was correlated with the acoustic biomass in the previous year.

The observed length-compositions of krill showed a regular pattern of small krill recruiting to the survey approximately every 6 years (Fig. 3). The dashed vertical lines in Fig. 3 and subsequent figures drawn at 1996, 2002, and 2007 indicate the approximate beginning of each cycle of mostly smaller krill followed by larger krill in succeeding years.

3.2. Effects of different selectivities and biomass indices on the estimates

All eight model configurations based on time-constant selectivities produced invertible Hessian matrices. Many randomized phase reorderings were typically required before obtaining an invertible Hessian, particularly for the more complex configurations fitted to both biomass indices assuming double-logistic selectivities. The eight annually varying configurations did not produce Hessian matrices after several thousand randomized phase reorderings.

The AIC scores for the time-constant configurations were much lower (better) than the scores for the annually varying configurations fitted to the same data. The lowest AIC score (70.01) for the configurations using both biomass indices was for the "b-ll" configuration with time-constant, logistic selectivities (Table 5). The lowest AIC score for the configurations with annually varying selectivities fitted to both biomass indices (226.65) was also for the "b-ll" configuration.

Steepness was estimated to be 1 for most configurations, indicating either high productivity at low spawning biomass, or that this parameter could not be estimated (Table 5). The sole exception was the annually varying "n-d" configuration, which estimated a very low steepness of 0.25 (not shown).

Length-at-age estimates displayed two slightly different patterns among configurations. Twelve of the configurations produced the same pattern estimated by the "b-ll" model with time-constant selectivity (Fig. 4a). The annually varying "b-ld", "b-dd", "n-d" and time-constant "b-dl" configurations estimated an alternative pattern of slower growth (Fig. 4b).

The configurations with time-constant selectivities estimated similar time-series patterns for total and spawning biomasses, although the absolute scaling differed depending on which biomass indices were fitted (Fig. 5a, Table 5). The lowest estimates of mean annual total biomass for the population supplying the U.S. AMLR sampling area during the 20-year period were from the configurations using only the biomass indices from nets (~1.5 mt in the net-only configuration with the lowest AIC), followed by those using only the acoustic indices (~11.8 mt). The highest estimates were produced by the configurations that were fitted to both indices (~114 mt) (Table 5).

Three of the four time-constant configurations fitted to both biomass indices produced similar time-series patterns (Fig. 5a). The exception was the "b-dl" configuration (lowest solid lines for total and spawning biomass in Fig. 5a), which displayed different variability through time than the other configurations, and was closer in scaling to the estimates based only on acoustic indices than to the other configurations fitted to both nets and acoustics.

The configurations with annually varying selectivities usually estimated total and spawning biomasses lower than the time-constant configurations. The annually varying models also had a

Table 5
Estimates from different model configurations in Table 3 of mean annual total biomass, spawning biomass, recruitment, "mortality", AIC score and likelihood component values ("acoustics", "nets", "compositions", and "penalties"), and densities if all the biomass was assumed to occur inside the U.S. AMLR study area or disbursed throughout the Scotia Sea. Configurations are ordered by increasing value for mean total biomass. "Annually varying" column is "b-ll" configuration with annually varying selectivity, all others are time-constant.

Configuration[a]	n-d	n-l*	Annually varying	b-dl	a-d	a-l*	b-dd	b-ld	b-ll*
$\bar{B}(10000\,t)$	142	147	485	599	807	1180	5780	9220	11,400
Sp. $\bar{B}(10000\,t)$	38	36.4	144	377	228	291	1480	2320	2700
$\bar{R}(10000\,N_{age1})$	385	431	1280	288	2210	3850	16,400	27,100	35,700
M + emigration	1.011	1.062	0.9909	0.372	1.02	1.126	1.041	1.06	1.101
h	0.999	0.999	0.999	0.999	0.999	0.999	0.999	0.999	0.999
q acoustics	NA	NA	1	1	1	1	1	0.999	1
q nets	1	1	0.28	0.075	NA	NA	0.023	0.0205	0.015
Parameters	43	41	120	46	43	41	48	46	44
AIC[b]	68.02	64.02	226.65	73.99	68.01	64.01	78.01	74.01	70.01
Acoustics	NA	NA	0.08434	41.986	45.436	46.096	34.323	34.87	34.576
Nets	14.746	14.38	6.962	10.827	NA	NA	16.265	16.09	16.123
Compositions	7977	7981	7926	8050	7971	7977	7978	8073	7978
Penalties	43.429	43.686	8.574	51.799	51.211	50.615	46.53	45.95	46.469
g m^{-2} U.S. AMLR	11.362	11.736	38.77	47.883	64.516	94.142	462.678	737.4	914.405
g m^{-2} Scotia Sea	0.688	0.71	2.347	2.899	3.905	5.699	28.008	44.64	55.353

[a] An asterisk indicates the configuration with the lowest (best) AIC value for a given set of input data with time-constant selectivity.
[b] AIC values of configurations using different data (net only, acoustic only, both combined) are not comparable.

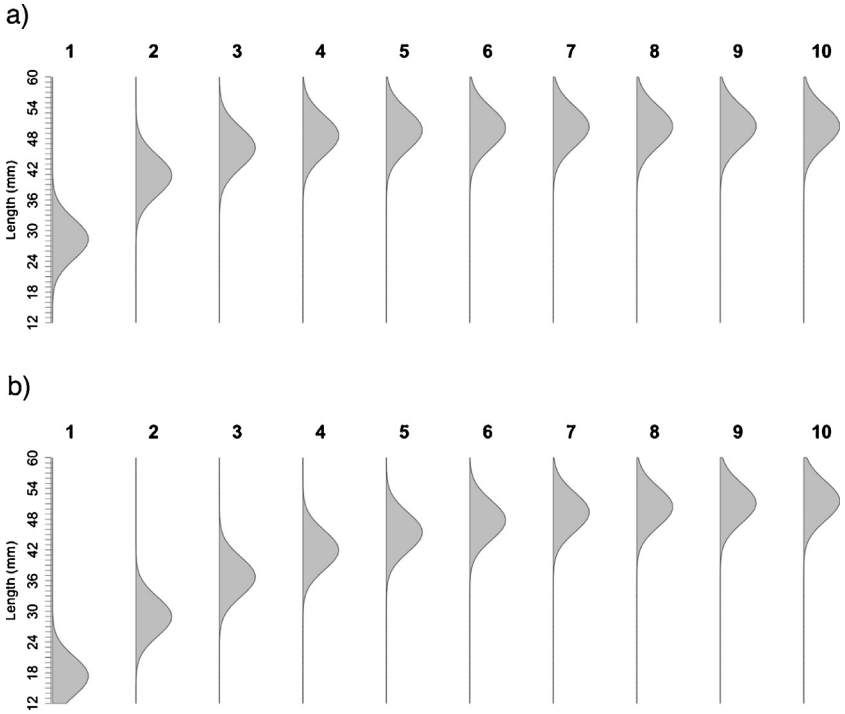

Fig. 4. Krill age-length growth estimates in mm for ages 1 to 10. (a) Twelve of the model configurations estimated growth as shown. (b) Four configurations, the time-varying "b-ld", "b-dd" and "n-d", and the time-constant "b-dl" models, estimated slower growth.

smaller overall range and less consistent time-series patterns in the biomass estimates among configurations (Fig. 5b). These configurations fitted the biomass indices much better than the time-constant models, as expected (Fig. 6). The "b-ll" configuration with annually varying selectivity estimated lower population biomass than any of the time-constant models fitted to both biomass indices (Table 5). All the other annually varying configurations produced population estimates (not shown) within the range of values provided in Table 5 except for the "n-l" configuration at 1.38 million tons, just below the minimum estimate of 1.42 million tons from the configurations with time-constant selectivity.

The annual mean total biomass of 114 million tons in the time-constant "b-ll" configuration represents an average density of 914 g m^{-2} if it is all located inside the U.S. AMLR survey area or 55 g m^{-2} if the population is located throughout the Scotia Sea (Table 5). These estimates include krill biomass of ages unobserved by the surveys due to selectivity.

The models also estimated the biomasses of krill that were available to each annual survey given the selectivity of that survey. The point estimate of biomass from the CCAMLR 2000 Survey transects conducted inside the U.S. AMLR survey area was higher than the point estimates of the U.S. AMLR surveys in all years. All the models estimated that the biomass available to acoustic observation in the year 2000 was less than that calculated from the CCAMLR 2000 Survey data, as illustrated for the "b-ll" configuration (Fig. 6).

The selectivities estimated by the time-constant configurations using both biomass indices displayed similar patterns, especially for younger krill (Fig. 7). All configurations estimated low selectivities by acoustics for krill less than 4 years of age, rapidly increasing for krill older than 5 or 6 years of age. Higher selectivities by nets

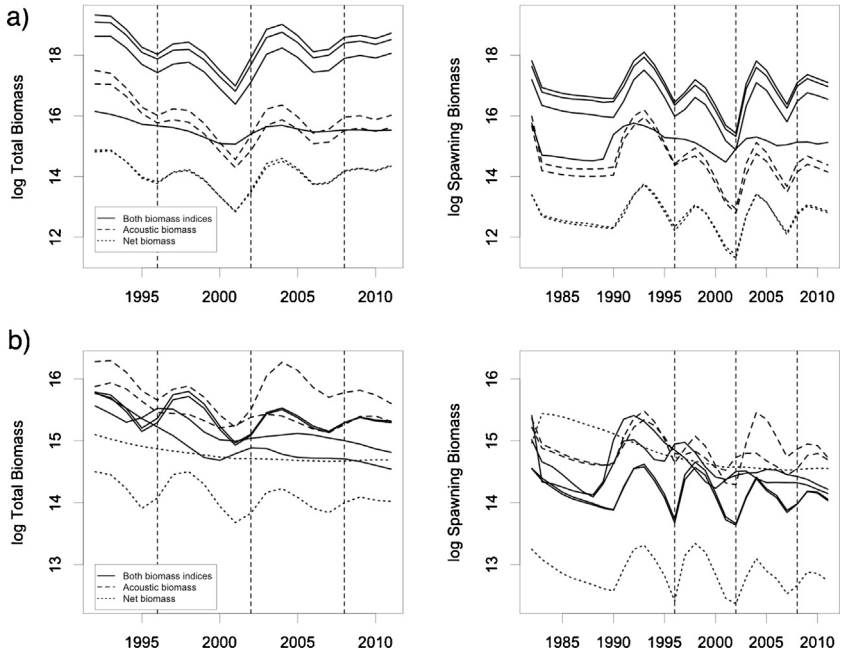

Fig. 5. Estimates of total (left plots) and spawning (right) krill biomass from 16 model configurations. Vertical dashed lines indicate years with high proportions of small krill (from Fig. 3). The spawning biomass figures include estimates for the pre-data years 1983–1991 while the estimates of total biomass begin with the first year of observations in 1992. Configurations fit to both biomass indices (solid lines), acoustic biomass only (dashes) and net biomass only (short dashes) are shown for (a) time-constant selectivities and (b) annually varying selectivities.

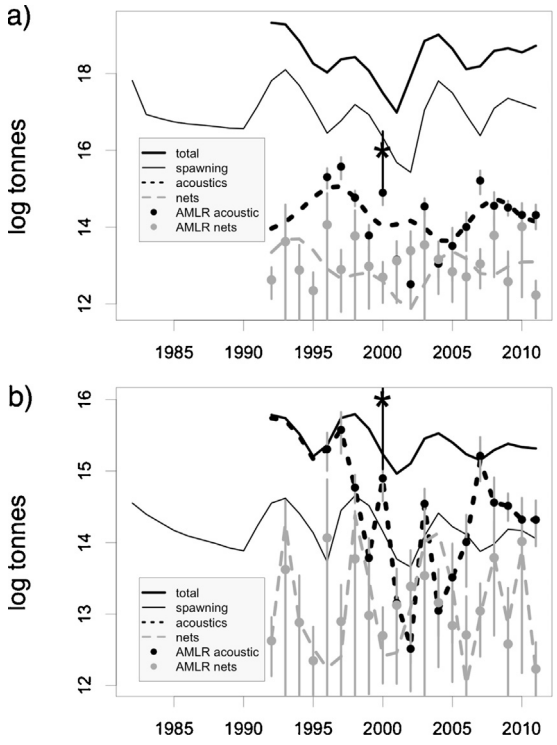

Fig. 6. Biomass estimates and fits to indices of the "b-ll" model configurations with (a) time-constant and (b) annually varying selectivities. U.S. AMLR survey biomass indices from acoustics (black points) and nets (gray points) are shown with plus and minus one standard error along with estimates of total krill biomass (top solid line), spawning biomass (lower solid line), biomass available to acoustics (top dark dashed line) and available to nets (bottom light dashed line). The CCAMLR 2000 Survey point estimate (asterisk) and 95% CI from transects completed inside the U.S. AMLR survey area are shown for comparison. Dashed vertical lines indicate years with high proportions of small krill (from Fig. 3).

for krill of younger ages were mediated by lower overall catchabilities, usually around 2%, relative to acoustics (Table 5). In the best fitting model with logistic selectivity for both the acoustic and net surveys ("b-ll"), acoustics selected mostly the oldest krill and nets selected a wider range of ages (Fig. 7a).

All configurations fitted the length-composition data with similar precision (see the row labeled "compositions" in Table 5 for the likelihood component values). The "b-ll" configuration illustrates the fit of the model to individual years of length-compositions (App. Fig. A.1).

3.3. Simulation testing

When fitted to simulated data, some model configurations were initially unable to reproduce the derived quantities of spawning biomass and recruitment that matched those from their respective operating models even though the operating models produced estimates of asymptotic variances and appeared to have invertible Hessians. For all configurations with time-constant selectivity, reordering the estimation phases within the operating or estimating models eventually yielded models that were able to both fit the "data" produced from the operating models and to reproduce the derived quantities of recruit abundance, spawning biomass, mortality, and steepness very closely.

Very small numerical errors due to pre-specified variances in the models using simulated data were present but not visible at the overall scale of measurement. This is illustrated for the "b-ll" configuration with time-constant selectivity for the length compositions (Fig. A.1b), biomass fits (Fig. 8a), and derived quantities of recruit abundance (Fig. 8b) and spawning biomass (Fig. 8c). The matches between operating and estimating models from the other seven configurations with time-constant selectivity (not shown) were equally close to those for the "b-ll" configuration.

Four models with annually varying selectivity failed to fit all the simulated data precisely or to closely reproduce the derived quantities for spawning biomass and recruitment. These were the "b-dl", "b-dd", "a-d" and "n-d" configurations (the "b-ll", "b-ld", "a-l", and

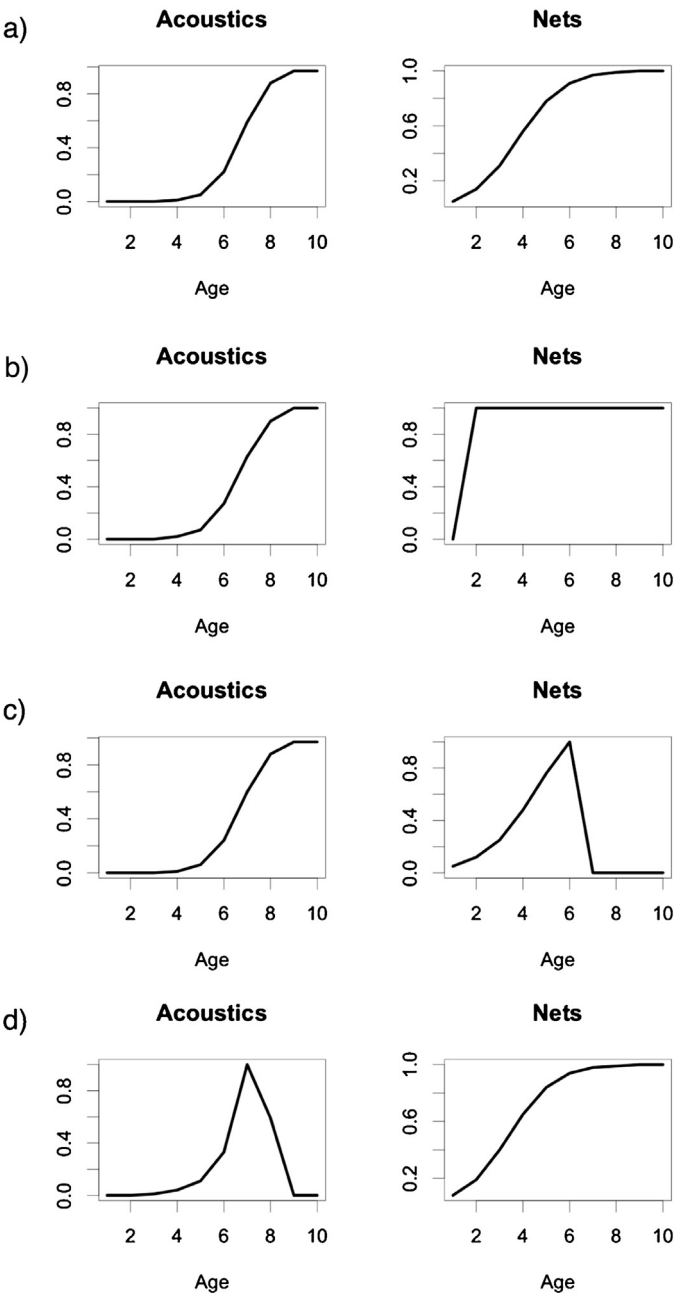

Fig. 7. Estimated selectivities from configurations fitted to both biomass indices but assuming different time-constant forms as noted. Configurations are ordered from lowest to highest AIC. (Table 5). (a) "b-ll"; (b) "b-dl"; (c) "b-ld" and; (d) "b-dd" configurations.

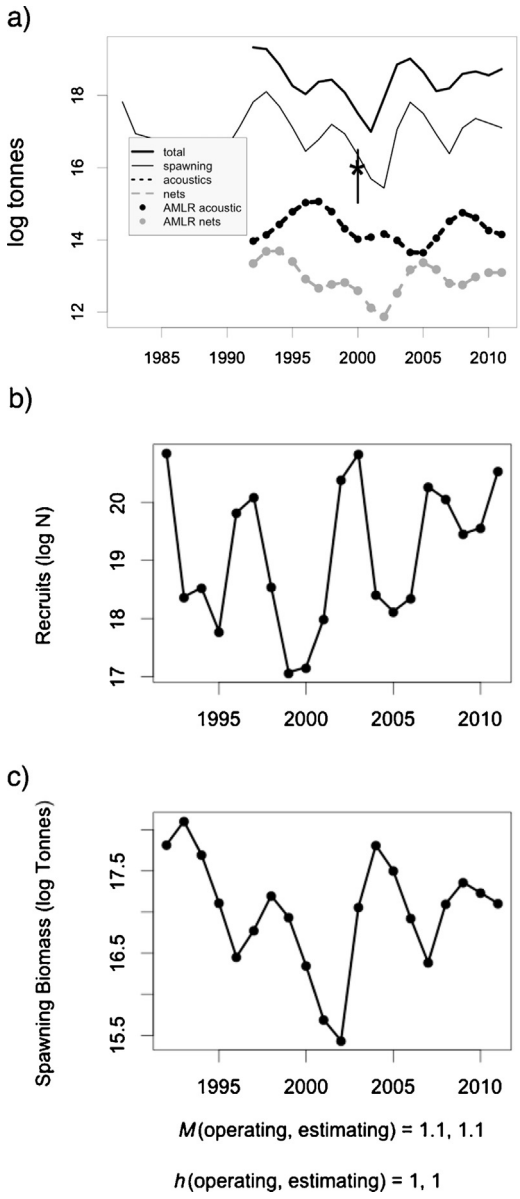

Fig. 8. Fits of the time-constant "b-ll" configuration to simulated acoustic and net data, and matches of estimates of derived quantities to the operating model. (a) Biomass data from operating model (points), estimating model estimates (lines), CCAMLR 2000 biomass estimate (asterisk); (b) match of estimated recruit abundance (lines) with operating model (points); (c) match of estimated spawning biomass with operating model, and operating model ("orig") and estimating model ("sim") estimates for mortality (M) and steepness (h).

"d-l" configurations were able to reproduce the derived quantities even though they did not produce invertible Hessian matrices). The fits for the "b-dd" configuration illustrate these problems (Fig. 9). This configuration was unable to produce model estimates that matched the derived quantities or even to precisely fit the simulated biomass (Fig. 9a) and composition data. The estimates for mortality (M) and steepness (h) also failed to match between the operating and estimating models with annually varying double-logistic selectivity (Fig. 9c).

Markov chain Monte Carlo sampling indicated that three of the four configurations fitted to both biomass indices with time-constant selectivity produced essentially identical probability distributions for spawning biomass, recruit abundance, and mortality (Fig. 10). The estimates from the "b-dl" configuration continued to be anomalous compared to the other three configurations, as was reported for the maximum posterior density estimates of growth, biomass and other parameters of this configuration. Even though estimates of asymptotic variances were obtainable using this "b-dl" configuration, the Metropolis–Hastings algorithm was unsuccessful in obtaining a wide sampling of the distribution even after 5,000,000 MCMC samples, as indicated by the lack of variability around the estimates (Fig. 10b).

4. Discussion

The two-stage procedure of first randomizing the phase order until a positive definite Hessian matrix was obtained and then verifying the model estimates using simulated data allowed more complex combinations of models with data to be explored in this

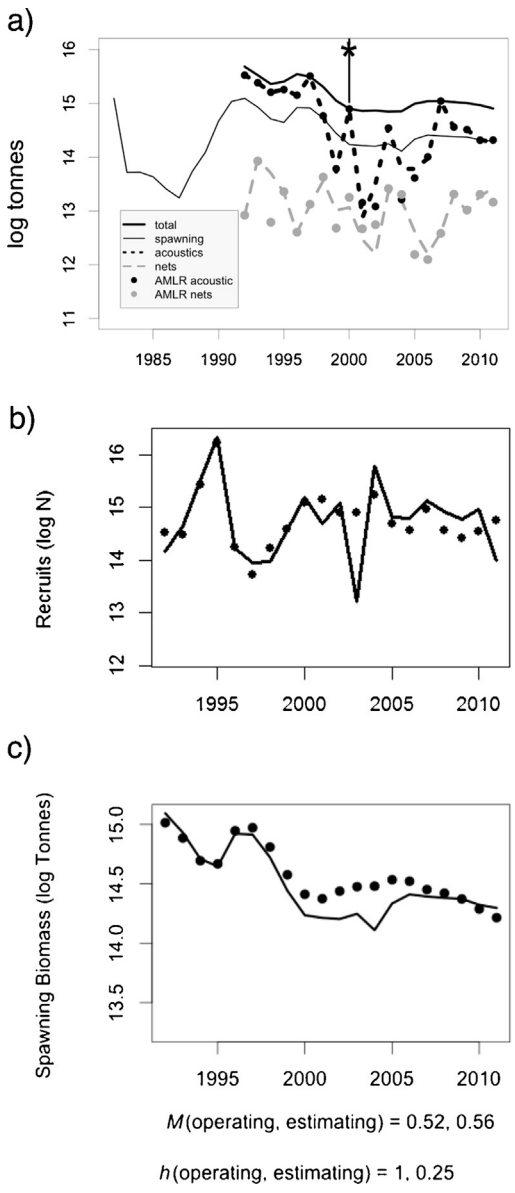

Fig. 9. Fits of the annually varying "b-dd" configuration to simulated acoustic and net data, and matches of estimates of derived quantities to the operating model. (a) Biomass data from operating model (points), estimating model estimates (lines), CCAMLR 2000 biomass estimate (asterisk); (b) match of estimated recruit abundance (lines) with operating model (points); (c) match of estimated spawning biomass with operating model, and operating model ("orig") and estimating model ("sim") estimates for mortality (M) and steepness (h).

study than would be possible using only a single, pre-specified phase order. Developers of any integrated stock assessment who are having trouble obtaining a converged model might consider using the procedures employed in this study. We note, however, that more experience using this approach may be needed to better understand why some phase orders "work" when others do not.

The second stage of comparing the parameter estimates to those of the operating model demonstrated that internally consistent representations of krill population dynamics had been obtained. The need to iterate the procedure until the estimates of the generating and simulation-based models matched indicated that discriminating between local and global minima in the negative log-likelihood surface was an issue for achieving convergence using these complex models and the data for Antarctic krill used here.

As model and data complexity increased from one biomass index to two, from logistic to double-logistic selectivity, and from time-constant to annually varying selectivity, the number of phase randomizations and the time required to produce consistent models typically increased. The simplest models with a single biomass index and time-constant selectivities often produced positive definite Hessian matrices and matched the estimates from the operating models after only a few phase randomizations. The most complex models with double-logistic, annually varying selectivities were unable to match the operating model estimates, even after thousands of trials with randomized phases processing over several days. While it is possible that applying more phase randomized trials to the models that failed would eventually find a generating model with an invertible Hessian matrix that also matched derived values from the operating model, the double-logistic, annually varying models were clearly a challenge, at least, to generating reproducible estimates of derived quantities.

Decisions about which potential sources of data to fit in stock assessments are made outside of formal model selection procedures. Since there is no reason in this case to select one biomass index over the other, models integrating both net and acoustic biomass indices with the size compositions from research net tows are currently proposed as the best option for modeling krill. Of the configurations using both biomass indices, the one with time-constant, logistic acoustic and net selectivities (the "b-ll" configuration) was the best model based on the AIC score (Table 5).

Based on the AIC, all the models using time-constant selectivities were superior to those fitted to the same data but allowing annually varying selectivities. The time-constant configurations also produced invertible Hessian matrices and hence asymptotic variance estimates, and were all able to reproduce the operating model estimates using simulated data.

As noted by Maunder and Harley (2011), it is not surprising that models with several parameters for selectivity each year are not selected by AIC over models with only several parameters over the entire time series. Maunder and Harley (2011) used a non-parametric method of estimating annually varying selectivity with a coefficient for each year and differences between coefficients smoothed by a penalty function chosen using cross-validation. The appropriate smoothness value was based on the ability to predict derived parameters for a test data set estimated from a separate training set of data. Such a non-parametric approach to modeling time-varying selectivity might result in fewer parameters and better model performance for time-varying selectivity than the parametric forms used in this study.

A basic issue in integrated fisheries assessment modeling is how much emphasis to place on the size- or age-composition data versus on the biomass indices (e.g. Francis, 2011). Lee et al. (2014) suggest using likelihood profiling on a scaling parameter such as unfished recruitment, R_0, to evaluate the effect of different likelihood components on the overall scaling of a stock assessment. They recommend allowing selectivity to vary with time if the composition data are having an undue influence relative to the abundance (or biomass) data. Time-varying selectivity essentially down-weights the influence of the composition data on the parameter estimates by allowing many more free parameters in fitting this data source. This suggestion follows the rule-of-thumb offered by Francis (2011) to fit the abundance data in a stock assessment preferentially over the compositions. In some cases, however, such as the simulation study by Wang et al. (2014), length-composition data can provide useful information about scaling parameters such as R_0. Indeed, likelihood profiling (not shown) of the eight configurations of the krill model with time-constant selectivities indicated that the effect of the survey biomass indices was flat for the estimate of R_0 across orders of magnitude and that the composition data were having a stronger influence on the estimate for R_0.

The fundamental question regarding size-composition data and their influence on the estimates of population scale is whether

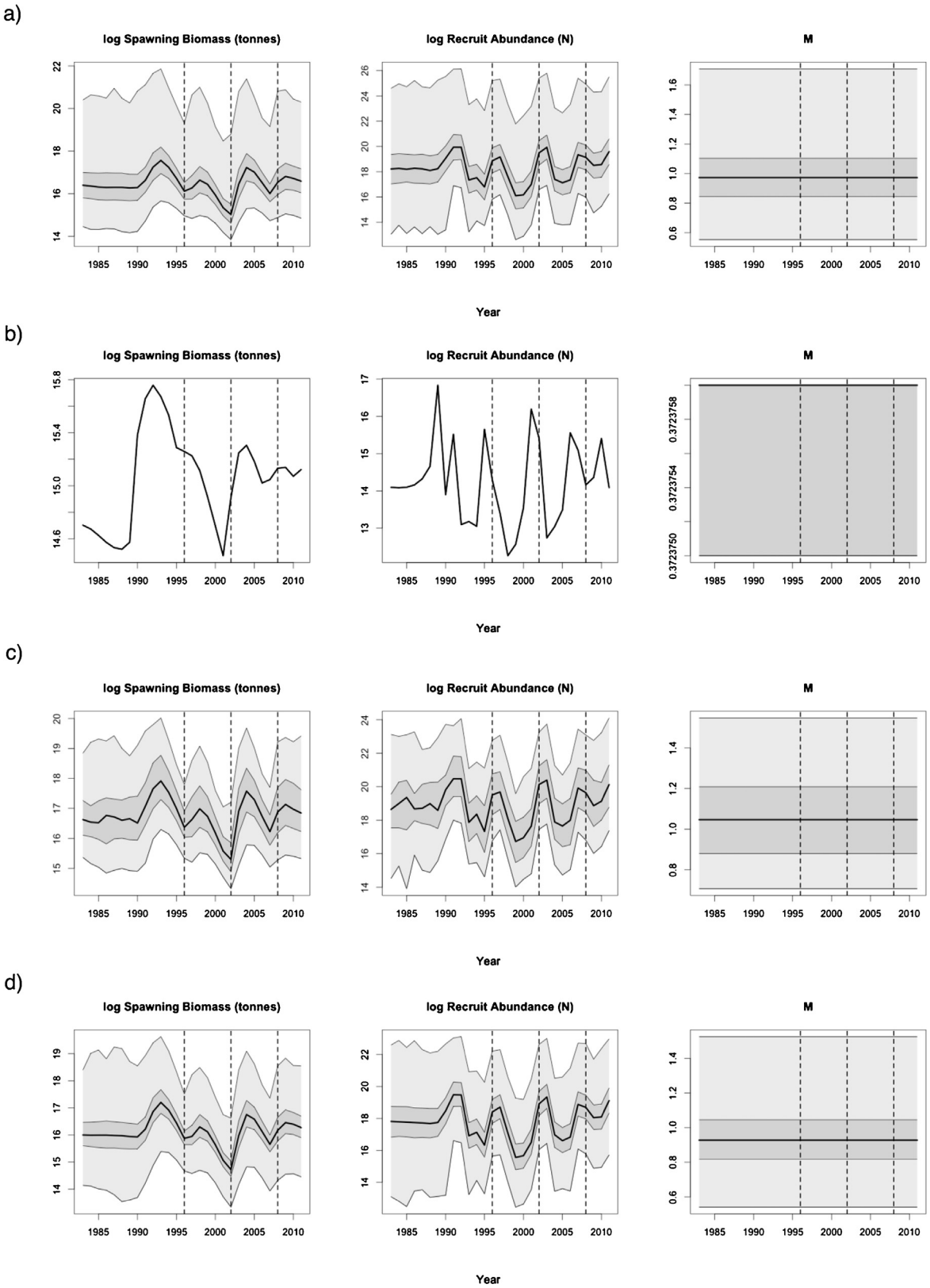

Fig. 10. MCMC sampling distributions for spawning biomass, recruit abundance and mortality from the configurations using both biomass indices with time-constant selectivities. Configurations are ordered by AIC score. 0%, 25%, 50%, 75%, and 100% quantiles are shown.

the annual variability in size-compositions is a real feature of the population or a sampling artifact. Previous studies of Antarctic krill have indicated that annual changes in krill abundance from surveys using different methods in different parts of the Scotia Sea are related (Brierley et al., 1999), as are regional recruitment indices (Siegel et al., 2003). The overall variability in krill length-compositions sampled from predator diets in the Scotia Sea is similar to the variability of length-compositions in net surveys

(Reid et al., 1999; Kinzey et al., 2013). These findings indicate that the annual variability observed in the length-composition data is a real population attribute. Therefore, down-weighting these compositions is, in this case, unwarranted. Careful consideration needs to be given to the data sources available to an assessment before increasing the influence of one source at the expense of another.

The MCMC samples of the estimates for spawning biomass, recruitment, and mortality of the "b-dl" configuration diverged from the pattern evident in the other three configurations with time-constant selectivity fitted to both biomass indices (Fig. 10). The "b-dl" configuration apparently settled into a local but not global minimum. This can be seen by comparing the sums of the likelihood component values of the "b-dl" with the "b-ll" configuration (rows labeled "acoustics", "nets", "compositions", and "penalties" from Table 5). The "b-dl" configuration had a larger absolute negative log-likelihood (8155) than the "b-ll" configuration (8075). Yet the "b-dl" configuration, with more flexible selectivity parameters, should have been able to produce selectivities that resulted in the same or better total objective value as the "b-ll" configuration. This indicates that being able to successfully produce asymptotic variance estimates and reproduce derived parameters by fitting to simulated data is not always sufficient to verify that the best possible parameter estimates have been achieved in such complex models.

Size-structured modeling is an alternative to age-structured modeling in fisheries stock assessment (Punt et al., 2013). Many size-structured methods, such as length-converted catch curves (e.g., Pauly, 1990) require the assumption of constant recruitment at equilibrium. This assumption is not met by Antarctic krill, whose natural recruitment variability has been described as "episodic" (Quetin and Ross, 2003). Other size-structured methods make use of mark-recapture data to estimate size-transition matrices. Mark-recapture methods are currently impractical for very small, superabundant, mobile organisms such as Antarctic krill. An age-structured approach is appropriate for Antarctic krill because the highly variable recruitment signal in length frequencies (Fig. 3) provides the information required to follow annual cohorts and to estimate the length distribution at each age.

The method of estimating growth used in these models is based on fitting trends in the observed length distributions. There is no information on potentially time-varying growth that is available for the models to use, as would be the case if for example, there were independent measures of length-at-age, so the potential for time-varying growth was not explored.

Work on the krill assessment model is ongoing. The next stage of model development is to incorporate the fisheries-dependent data into the modeling framework along with the ability to make forward projections so that potential fishing scenarios can be compared to the CCAMLR decision rules.

A conceptual inconsistency in this study is that the acoustic processing uses the distorted-wave Born approximation, in which size distributions taken from the nets are used in processing the backscatter data to produce the acoustic biomass index supplied to the models (Demer and Conti, 2003a,b,c,d; Reiss et al., 2008; CCAMLR, 2010; Fielding et al., 2011). This seems contrary to nets and acoustics having different selectivities for krill. A better approach for the future could be to remove the net information from the acoustic processing before it is supplied to the model and, instead, use the integrated model to resolve the sizes observed in the nets with the acoustic signal through the time series.

Acknowledgments

We thank our colleagues at the U.S. Antarctic Marine Living Resources Program who conducted the acoustic and net surveys for over two decades that provided the data on which this paper is based. Volker Siegel and Valerie Loeb were instrumental in supplying expertise in the initial design and implementation of the field surveys. Discussions with Jason Cope, Kevin Hill and Doug Butterworth, and the comments of three anonymous reviewers, helped clarify some aspects regarding the estimation of steepness and catchability, the use of size-data from nets in processing the acoustic data when selectivities differ, and related issues in this study. Two workshops hosted by the Center for the Advancement of Population Assessment Methodology (CAPAM) from March 11–14, 2013 and November 3–6, 2014 in La Jolla, CA, USA, provided the initial impetus for this paper.

Appendix A. Supplementary data

Supplementary data associated with this article can be found, in the online version, at http://dx.doi.org/10.1016/j.fishres.2015.03.023

References

Atkinson, A., Siegel, V., Pakhomov, E.A., Jessopp, M.J., Loeb, V., 2009. A re-appraisal of the total biomass and annual production of Antarctic krill. Deep Sea Res. Part I 56, 727–740.

Burnham, K.P., Andersen, D.R., 1998. Model Selection and Inference: A Practical Information-Theoretic Approach. Springer-Verlag, New York, pp. 353.

Brierley, A.S., Demer, D.A., Watkins, J.L., Hewitt, R.P., 1999. Concordance of interannual fluctuations in acoustically estimated densities of Antarctic krill around South Georgia and Elephant Island: biological evidence of same-year teleconnections across the Scotia Sea. Mar. Biol. 134, 675–681.

Brierley, A.S., 2008. Antarctic ecosystem: are deep krill ecological outliers or portents of a paradigm shift? Curr. Biol. 18 (6), 252–254.

CCAMLR, 2010. Report of the Fifth Meeting of the Subgroup on Acoustic Survey and Analysis Methods. SC-CCAMLR-XXIX/6, pp. 187–191. www.ccamlr.org/en/sc-camlr-xxix

Clarke, A., Tyler, P.A., 2008. Adult Antarctic krill feeding at abyssal depths. Curr. Biol. 18, 282–285.

Constable, A.J., de la Mare, W.K., 1996. A generalised model for evaluating yield and the long-term status of fish stocks under conditions of uncertainty. CCAMLR Sci. 3, 31–54.

Constable, A.J., Williamson, A.T., de la Mare, W.K., 2003. Generalised Yield Model: User's Manual and Specifications. Version 5.01b. Australian Antarctic Division, Kingston, Australia, pp. 165, http://www.antarctica.gov.au/science/southern-ocean-ecosystems-environmental-change-and-conservation/southern-ocean-fisheries/fish-and-fisheries/conservation-and-management/generalised-yield-model

Demer, D.A., Conti, S.G., 2003a. Validation of the stochastic distorted-wave Born approximation model with broad bandwidth total target strength measurements of Antarctic krill. ICES J. Mar. Sci. 60, 625–635.

Demer, D.A., Conti, S.G., 2003b. Reconciling theoretical versus empirical target strengths of krill: effects of phase variability on the distorted-wave Born approximation. ICES J. Mar. Sci. 60, 429–434.

Demer, D.A., Conti, S.G., 2003c. Erratum. ICES J. Mar. Sci. 61, 155–156.

Demer, D.A., Conti, S.G., 2003d. Erratum. ICES J. Mar. Sci. 61, 157–158.

Deroba, J.J., 34 others, 2015. Simulation testing the robustness of stock assessment models to error: some results from the ICES strategic initiative on stock assessment methods. ICES J. Mar. Sci. 72 (1), 19–30.

Everson, I., 1982. Diurnal variations in mean volume-backscattering strength of an Antarctic krill (*Euphausia superba*) patch. J. Plankton Res. 4, 155–162.

Fielding, S., Griffiths, G., Roe, H.S.J., 2004. The biological validation of ADCP acoustic backscatter through direct comparison with net samples and model predictions based on acoustic-scattering models. ICES J. Mar. Sci. 61 (2), 184–200.

Fielding, S., Watkins, J., Cossio, A., Reiss, C., Watters, G., Calise, L., Skaret, G., Takao, Y., Zhao, X., Agnew, D., Ramm, D., Reid, K., 2011. The ASAM 2010 Assessment of Krill Biomass for Area 48 from the Scotia Sea CCAMLR 2000 Synoptic Survey. Document WG-EMM-11/20. CCAMLR, Hobart, Australia (Document available from corresponding author upon request).

Fielding, S., Watkins, J.L., Collins, M.A., Enderlein, P., Venables, H.J., 2012. Acoustic determination of the distribution of fish and krill across the Scotia Sea in spring 2006, summer 2008 and autumn 2009. Deep Sea Res. Part II 59–60, 173–188.

Fournier, D.A., Skaug, H.J., Ancheta, J., Ianelli, J., Magnusson, A., Maunder, M.N., Nielsen, A., Sibert, J., 2012. AD Model Builder: using automatic differentiation for statistical inference of highly parameterized complex nonlinear models. Optim. Methods Softw. 27, 233–249.

Francis, R.I.C.C., 2011. Data weighting in statistical fisheries stock assessment models. Can. J. Fish. Aquat. Sci. 68, 1124–1138.

Hewitt, R.P., Demer, D.A., 1996. Lateral target strength of Antarctic krill. ICES J. Mar. Sci. 53, 297–302.

Hewitt, R.P., Demer, D.A., Emery, J.H., 2003. An 8- year cycle in krill biomass density inferred from acoustic surveys conducted in the vicinity of the South Shetland

Islands during the austral summers of 1991/1992 through 2001/2002. Aquat. Living Resour. 16, 205–213.
Hewitt, R.P., Watkins, J., Naganobu, M., Sushin, V., Brierley, A.S., Demer, D., Kasatkina, S., Takao, Y., Goss, C., Malyshko, A., Brandon, M., Kawaguchi, S., Siegel, V., Trathan, P., Emery, J., Everson, I., Miller, D., 2004. Biomass of Antarctic krill in the Scotia Sea in January/February 2000 and its use in revising an estimate of precautionary yield. Deep Sea Res. Part II 51, 1215–1236.
Hofmann, E.H., Hüsrevoğlu, Y.S., 2003. A circumpolar modeling study of habitat control of Antarctic krill (*Euphausia superba*) reproductive success. Deep Sea Res. Part II 50, 3121–3142.
Jolly, G.M., Hampton, I., 1990. A stratified random transect design for acoustic surveys of fish stocks. Can. J. Fish. Aquat. Sci. 47, 1282–1291.
Kinzey, D., Watters, G., Reiss, C.S., 2013. Effects of recruitment variability and natural mortality on generalised yield model projections and the CCAMLR decision rules for Antarctic krill. CCAMLR Sci. 20, 81–96.
Lee, H.-H., Maunder, M.N., Piner, K.R., Methot, R.D., 2011. Estimating natural mortality within a fisheries stock assessment model: an evaluation using simulation analysis based on twelve stock assessments. Fish. Res. 109, 89–94.
Lee, H.-H., Piner, K.R., Methot, R.D., Maunder, M.N., 2014. Use of likelihood profiling over a global scaling parameter to structure the population dynamics model: an example using blue marlin in the Pacific Ocean. Fish. Res. 158, 138–146.
Maunder, M.N., Harley, S.J., 2011. Using cross validation model selection to determine the shape of nonparameteric selectivity curves in fisheries stock assessment models. Fish. Res. 110, 283–288.
Nicol, S., 2006. Krill, currents, and sea ice: *Euphausia superba* and its changing environment. Bioscience 56 (2), 111–120.
Nicol, S., Foster, J., Kawaguchi, S., 2012. The fishery for Antarctic krill – recent developments. Fish Fish. 13, 30–40.
Pauly, D., 1990. Can we use traditional length-based fish stock assessment when growth is seasonal? ICLARM Fishbyte 8, 29–32.
Punt, A.E., Huang, T.C., Maunder, M.N., 2013. Review of integrated size-structured models for stock assessment of hard-to-age crustacean and mollusk species. ICES J. Mar. Sci. 70 (1), 16–33.
Quetin, L.B., Ross, R.M., 2003. Episodic recruitment in Antarctic krill *Euphausia superba* in the Palmer LTER study region. Mar. Ecol. Prog. Ser. 259, 185–200.
Reid, K., Watkins, J.L., Croxall, J.P., Murphy, E.J., 1999. Krill population dynamics at South Georgia 1991–1997, based on data from predators and nets. Mar. Ecol. Prog. Ser. 177, 102–114.
Reiss, C.S., Cossio, A.M., Loeb, V., Demer, D.A., 2008. Variations in the biomass of Antarctic krill (*Euphausia superba*) around the South Shetland Islands, 1996–2006. ICES J. Mar. Sci. 65, 497–508.
Schmidt, K., Atkinson, A., Steigenberger, S., Fielding, S., Lindsay, M.C., Pond, D.W., Tarling, G.A., Klevjer, G.A., Allen, C.S., Nicol, S., Achterberg, E.P., 2011. Seabed foraging by Antarctic krill: implications for stock assessment, benthopelagic coupling, and the vertical transfer of iron. Limnol. Oceanogr. 56, 1411–1428.
Siegel, V., Loeb, V., 1995. Recruitment of Antarctic krill *Euphausia superba* and possible causes for its variability. Mar. Ecol. Prog. Ser. 123, 45–56.
Siegel, V., Ross, R.M., Quetin, L.B., 2003. Krill (*Euphausia superba*) recruitment indices from the western Antarctic Peninsula: are they representative of larger regions? Polar Biol. 26, 672–679.
Siegel, V., 2005. Distribution and population dynamics of *Euphausia superba*: summary of recent findings. Polar Biol. 29, 1–22.
Siegel, V., Reiss, C.S., Dietrich, K.S., Haraldsson, M., Rohardt, G., 2013. Distribution and abundance of Antarctic krill (*Euphausia superba*) along the Antarctic Peninsula. Deep Sea Res. Part I 77, 63–74.
Trathan, P.N., Watkins, J.L., Murray, A.W.A., Brierley, A.S., Hewitt, R., Demer, D., Naganobu, M., Kawaguchi, S., Sushin, V., Kasatkina, S.M., Hedley, S., Kim, S., Pauly, T., 2001. The CCAMLR-2000 krill synoptic survey: a description of the rational and design. CCAMLR Sci. 8, 1–23.
Wang, S.P., Maunder, M.N., Piner, K.R., Aires-da-Silva, A., Lee, H.H., 2014. Evaluation of virgin recruitment profiling as a diagnostic for selectivity curve structure in integrated stock assessment models. Fish. Res. 158, 158–164.
Wiebe, P., Ashjian, C., Gallager, S., Davis, C., Lawson, G., Copley, N., 2004. Using a high powered strobe light to increase the catch of Antarctic krill. Mar. Biol. 144 (3), 493–502.
Wiebe, P., Ashjian, C., Gallager, S., Lawson, G., Piñones, A., Copley, N., 2011. Horizontal and vertical distribution of euphausiid species on the Western Antarctic Peninsula U.S. GLOBEC Southern Ocean Study site. Deep Sea Res. Part II 58, 1630–1651.